Interactions between Keggin-Type Lacunary Polyoxometalates and Ag Nanoparticles: A Surface-Enhanced Raman Scattering Spectroscopic Investigation*

Georgeta C. Lica,[1] **Kevin P. Browne,**[1] **and YuYe Tong**[1,2]

Interactions between two Keggin-type lacunary polyoxometalates (POMs), $PW_{11}O_{39}^{7-}$ and $SiW_{11}O_{39}^{8-}$, and pre-formed citrate-protected colloidal Ag nanoparticles (NPs) were studied by surface-enhanced Raman scattering (SERS) and UV-Vis spectroscopies. Clear SERS evidence of displacing the originally surface-bound citrate ions by the subsequently added POMs indicates a stronger metal–ligand interaction between the POMs and the Ag NPs. Accompanied red-shifts in the surface plasma peak position of the Ag NPs were also observed for both POMs. The simultaneous presence of a number of SERS vibrational bands which can be assigned to vibrational modes of the POM molecule suggests that its overall structure is intact upon adsorption. Based on the SERS observations, a bonding between the penta-dentate aperture of the POMs and the Ag NP surface was proposed.

INTRODUCTION

Polyoxometalates (POMs) are an important and highly diversified class of inorganic molecules and/or stoichiometric clusters of early transition metal oxides [1]. Structurally speaking, they are formed by corner- and edge-sharing of the basic transition metal octahedron building block, MO_6, and usually possess high symmetry. As chemical species, their unique primary

*Dedicated to the retirement of Michael Pope.
[1]Department of Chemistry, Georgetown University, 37th & O Streets, NW, Washington, DC 20057, USA.
[2]To Whom Correspondence should be addressed. E-mail: yyt@georgetown.edu

structure results in many "value-adding" properties advantageous to processing that distinguish the POMs from metallic oxides and conventional compounds. These properties include diverse molecular composition and geometric shape, redox reversibility and tunable redox potentials, strong acidity, high solubility, and good structural stability and form the fundamental basis of their rich solution- and solid-state chemistry that leads to many important technological applications in fields such as catalysis, chemical sensing and charge transfer mediation, corrosion inhibition, medicine, and nuclear waste treatment, just to name a few [2].

More recently, much attention has been focused on using the POMs as surface modifiers for enhancing catalytic activity [3, 4] or inhibiting surface corrosion [5], or as protecting ligands for stabilizing metal nanoparticle (NP) [6–12]. It is worth noting that the POM modified electrodes are found not only to be very stable in solution over a wide pH range and in air, but be also electrochemically stable and insensitive to impurities and additives [13, 14]. However, the fundamentals of the relevant surface-based POM chemistry, i.e., the POM surface chemistry, has been much less vigorously investigated, probably due both to the complexity of the problems and the availability of investigative techniques [15]. Most recently, Gewirth, Klemperer, and their co-workers have pioneered investigations of the adsorption of POMs (in particular $SiW_{12}O_{40}^{4-}$ and $SiW_{11}O_{39}^{8-}$ anions) on single crystal Au and Ag surfaces with scanning tunneling microscope [16], specular X-ray reflectivity spectroscopy [17], and electrode potential dependent surface enhanced Raman scattering (SERS) spectroscopy [18, 19]. Evidence of strong POM–Ag interaction was found.

In this paper, we report the first SERS and UV-Vis spectroscopic investigation of the adsorption of two Keggin-type lacunary POMs, $PW_{11}O_{39}^{7-}$ and $SiW_{11}O_{39}^{8-}$, on citrate-protected colloidal Ag NPs. The observed high quality SERS spectra provide unambiguous evidence showing a complete displacement of the originally surface-bound citrate ions. This observation points to a stronger POM–Ag than citrate–Ag interaction. SERS spectroscopic evidence also suggests that the molecular structure of the POMs is intact upon adsorption and the POMs bind to the Ag NP surface via the penta-dentate aperture.

EXPERIMENTAL

The Ag NPs were synthesized following a modified version of the widely used Turkevich method [20] in which the $NaBH_4$ was used as the reducing agent. Briefly, a 100-ml solution of 2.5 mM $AgNO_3$ and 2.5 mM $Na_3Citrate$ was first prepared and stirred at room temperature for 1 h. About 4 ml of ice-cold $NaBH_4$ solution (0.1 M) was then added at once to

the vigorously stirred solution that resulted immediately in a dark brown solution which was further stirred for another 1/2 h. The Ag colloidal solution was then centrifuged for 45 min at 5000 rpm to remove the large aggregated NPs and improve the size distribution. The final solution had a dark yellow color and a pH of ca. 6–6.5. To this solution, a given amount of solid salt of $K_7PW_{11}O_{39}$ (the pH value of the colloidal Ag NP solution was adjusted to 5.5 with diluted H_2SO_4 before its addition in order to improve the structural stability) or $K_8SiW_{11}O_{39}$ was added to make the final concentrations of the POM ions be 2.5 mM for the former and 2.5 mM or 5 mM for the latter. The $AgNO_3$, $Na_3Citrate$ and $NaBH_4$ were purchased from Fisher and used without further purification. The POM salts were kindly provided by Dr. Pope. All the solutions were prepared with water purified by a Millipore Milli-Q Gradient A-10 system to 18.2 $M\Omega$.

All Raman spectra were taken with an Advantage 200A Raman spectrometer (Deltanu, Laramie, WY) with a 3-mW HeNe laser (633 nm wavelength) and nominal best resolution of 10 cm^{-1}. A medium resolution was used and an integration time was set to 20 s. All spectra were also baseline corrected. The UV-Vis measurements were performed using a single beam HP 8453 diode array UV-Vis spectrometer. All the samples were diluted 1/15 prior to the measurements.

RESULTS AND DISCUSSIONS

We present in Fig. 1A the SERS spectrum of the Ag NP surface-bound, protecting ligands of citrate before the addition of the POM potassium salts. All of the observed vibrational bands are in good agreement with previously published results [21, 22]. Particularly, the appearance of the band at 1025 cm^{-1} is the SERS fingerprint of the surface-bound citrate ions, although its assignment is still unknown. On the other hand, the strong band at 1398 cm^{-1} can be assigned to ν_s (COO) [22]. These observations are consistent with the presence of a protecting sheath of the citrate ions on the Ag NP surfaces. The inset is the UV-Vis spectrum of the Ag NPs' surface plasma resonance (SPR). Figure 1B provides the Ag NP size distribution measured by TEM and the inset is a representative transmission electron microscopic (TEM) image showing that the sizes of the majority NPs were between 1.5 and 5 nm although some agglomerations of the NPs were also observed on the TEM grids. Both the SPR peak position and the particle size confirm previously published results [22, 23].

The normal Raman spectra obtained on the solid salts of $K_7PW_{11}O_{39}$ (A) and $K_8SiW_{11}O_{39}$ (B) are shown in Fig. 2. The inset in Fig. 2A is a polyhedral representation of the Keggin-type lucunary structure where a WO unit is missing from the parent Keggin structure. Four types of oxygen
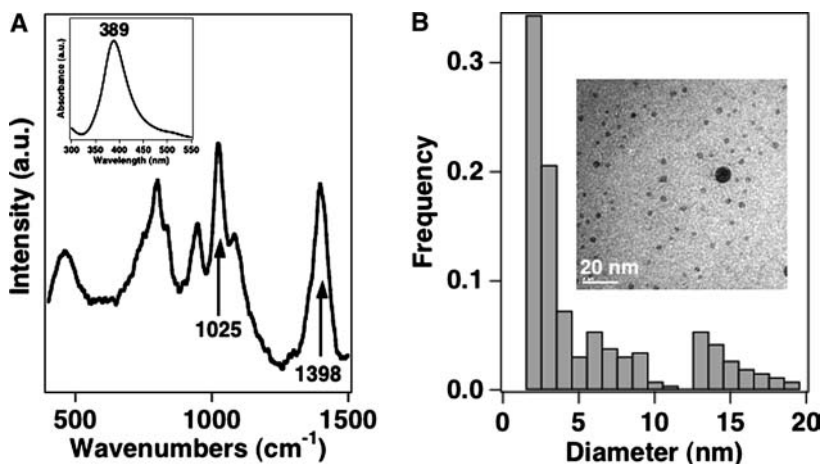
Fig. 1. (A) The SERS spectrum of the citrate ions adsorbed on the Ag NPs. The inset shows the UV-Vis SPR spectrum. (B) The Ag NP size distribution measured with TEM (262 total counts). The inset is a representative TEM image of the sample. The average particle size calculated from the size distribution is about 5.2 nm.
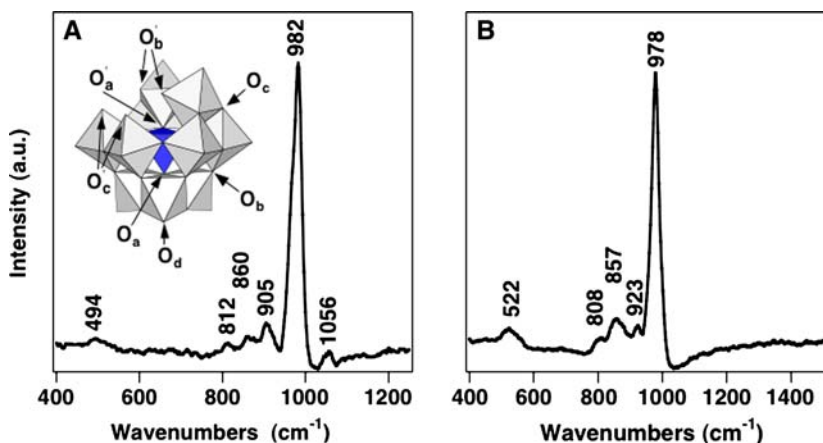

Fig. 2. The normal Raman spectra of the solid salts of $K_7PW_{11}O_{39}$ (A) and $K_8SiW_{11}O_{39}$ (B). When dissolved in aqueous solution, only the most intense bands were observed due to the limit of sensitivity and the peak positions were slightly red shifted. The inset in (A) is a cartoon representation of the Keggin-type lacunary structure. See text for the definitions of the symbols for different types of oxygen atoms.

atoms of the Keggin structure are identified: O_a is the oxygen atom bound to the heteroatom X, O_b is the corner-sharing (inter-triad) bridge oxygen atom, O_c is the edge-sharing (intra-triad) bridge oxygen, and O_d is the double bonded oxygen atom. The missing WO unit turns two O_b and two O_c into terminal-like oxygen atoms (indicated by O_b' and O_c') and exposes one O_a to the aperture (O_a'). These five oxygen atoms form a penta-dentate aperture of the lacunary POM and are believed to be the most active oxygen atoms of the molecule in terms of chemical bonding [1].

The vibrational bands observed in Fig. 2 are consistent with the literature values [19, 24]. The strongest band can be assigned to the $\nu_s(W = O_d)$ vibration. However, only a single band instead of a doublet was observed at 1056 cm^{-1} for $\nu_{as}(P–O_a)$ in $K_7PW_{11}O_{39}$ (most probably due to the resolution limit of the instrument) and whose intensity is about fifteen times smaller than that of the strongest band. Some general assignments of these bands are listed in Table 1. The literature values are from references 19 and 24 and listed in the parentheses.

In Fig. 3, we present the time-dependent SERS spectra (A) of the lacunary $PW_{11}O_{39}^{7-}$ anions (2.5 mM) adsorbing onto the Ag NP surfaces and the corresponding UV-Vis SPR spectra (B) of the Ag NPs. An almost complete displacement of the metal-surface-bound citrate ions by the adsorption of the $PW_{11}O_{39}^{7-}$ anions was observed right after their addition to the Ag NP solution, as evidenced by the quasi-disappearance of the citrate SERS peak at 1398 cm^{-1}. This indicates that the Ag NP–$PW_{11}O_{39}^{7-}$ bonding interaction is much stronger than that of Ag NP-citrate. Simultaneously, two strong SERS peaks appear at 967 and 790 cm^{-1}. We tentatively assign (*vide infra*) the former to the $\nu_s(W = O_d)$ and the latter to a combined contribution from the $\nu_{as}(W – O_b – W)$ and the $\nu_{as}(W – O_c – W)$. Additional bands were observed at 1015 and 576 cm^{-1} which are assigned to the $\nu_{as}(P – O_a)$ and

Table 1. Normal Raman and SERS Band Assignments (numbers in parentheses are from literature [19, 24])

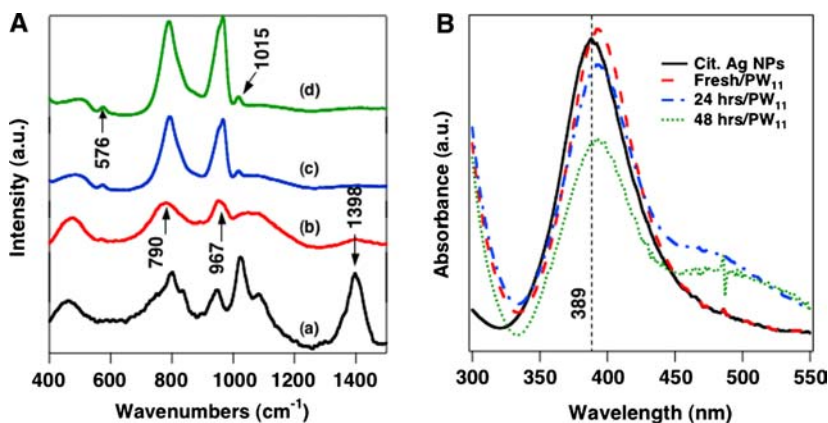| PW$_{11}$		SiW$_{11}$		
Peak Position (cm^{-1})		Peak Position (cm^{-1})		
Powder Raman	SERS	Powder Raman	SERS	Tentative Assignment
1056 (1085, 1040)	1015			$\nu_s(P–O_a)$
982 (979)	967	978 (973)	960 (971)	$\nu_s(W = O_d)$
		923 (923)		$\nu_s(W = O_d)$
860, 905	790	857 (865)	789 (795)	$\nu_{as}(W–O_b–W)$,
812		808 (805)		$\nu_{as}(W–O_c–W)$
494 (520, 500)	576	522 (524)		$\delta(W–O_{b(c)}–W)$

Fig. 3. The time-dependent SERS (A) and UV-Vis SPR (B) spectra of the Ag–citrate and Ag NP–$PW_{11}O_{39}^{7-}$ samples. A/B: (a)/solid curves: Ag-citrate; (b)/dashed curves: right after, (c)/dash-dotted curves: 24 hrs after, and (d)/dotted curves: 48 hrs after the addition of the PW_{11}.

$\delta(W - O_{b(c)} - W)$ vibrations respectively. Notice that the simultaneous observation of several SERS bands assignable to the POM molecule strongly suggests that the overall molecular structure of the absorbed POMs is intact.

An immediate corresponding red-shift (from 389 to 396 nm, Fig. 3B) in the surface plasma peak was also observed, again indicative of a strong POM–Ag interaction. It is interesting to note that the SERS signals continue to increase as time goes which was accompanied by the color change of the solution and the appearance of a broad surface plasma hump around 500 nm, as can be seen in Fig. 3B. This may be indicative of an on-going particles agglomeration that usually increases the enhancement factor of SERS.

Two most important features of SERS are probably the surface selection rules and the distance dependence. The former is a function of the excitation wavelength and for an excitation wavelength of 633 nm (the HeNe laser used here) theoretical calculations show that only the vibration modes perpendicular to the surface will be substantially enhanced [25]. For the latter, the most recent theoretical calculations for well-characterized NPs show that the enhanced electric fields decrease exponentially as the distance from the surface increases, with a characteristic length no larger than 2 nm [26]. With these SERS features in mind, we propose a bonding scheme between the POM's penta-dentate oxygen aperture and the Ag NP surface as illustrated in Fig. 4 to rationalize the observed POM SERS bands [27].
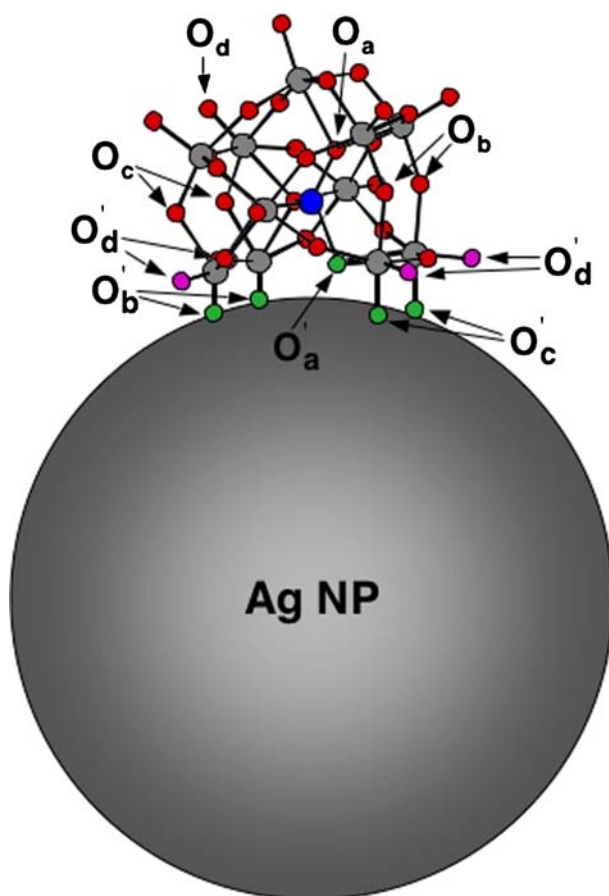
Fig. 4. A cartoon illustration of the bonding scheme between the lacunary POM and the Ag NP. The five oxygen atoms (two O_b's two O_c's, and one O'_a) that form the penta-dentate aperture and the four associated terminal oxygen atoms (O'_d) are indicated by arrows. Other types of oxygen atoms are also indicated for clarity.

Notice that the size of a Keggin POM is about 1 nm, which is comparable to the < 2 nm charateristic decay constant of SERS [26]. Therefore, it is expected that the SERS intensity for atoms at the top of the POM molecule would be noticeably weaker than those closer to the Ag NP surface. A rough estimate shows that the SERS enhancement for the $\nu_{as}(P–O_a)$ band at 1015 cm^{-1} is at least 10^3, a value that would put at least one of the O_a at a close proximity to the metal surface.

(The absolute intensity of this band is about two times larger than the strongest band of a 2.5 mM solution of the free POM which in turn is about 15 times stronger than the band at 1056 cm^{-1} (Fig. 2A). The average Ag NP size is about 5–6 nm which gives a dispersion of about 20%. The size of one POM would cover about 10 Ag surface atoms. Thus, only 2% of the added POMs are needed for a full coverage. Consequently, the SERS enhancement is approximately: $2 \times 15/2\% = 1500$.) Additionally, the band position is substantially redshifted compared to the value (1056 cm^{-1}) of the free $PW_{11}O_{39}^{7-}$ (Table 1), which suggests that the involved O_a have a direct interaction with the Ag NP surface. Clearly, these two observations support the bonding scheme proposed in Fig. 4.

The SERS $\nu_s(W{=}O_d)$ band at 967 cm^{-1} is also red-shifted with respect to that (982 cm^{-1}) of the free $PW_{11}O_{39}^{7-}$, again in consistence with a direct interaction between the involved terminal-like oxygen atoms and Ag NPs. We propose that this band comes mainly from the two O_b' and two O_d' that directly bind rather perpendicularly to the Ag NP surface. With this bonding scheme, the four O_d's associated with the bonding O_b's and O_d's would be forced to have their $W{=}O_d$ bonds largely parallel to the surface and thus would experience little SERS. The other 5 $W{=}O_d$ bonds are either already parallel to or quite far away from the surface, therefore, their contributions would be much smaller. The SERS band at 790 cm^{-1} is broader ($\Delta\nu \sim 100\,\mathrm{cm}^{-1}$) and covers the known spectral regions of $\nu_{as}(W{-}O_b{-}W)$ and the $\nu_{as}(W{-}O_c{-}W)$ (Table 1). It is also reasonable to believe that the strong POM–Ag bonding interaction through the penta-dentate aperture may distort to certain degree the molecular structure of the bound POMs and the intrinsic heterogeneity of this surface bonding can thus cause an overlap of the $\nu_{as}(W{-}O_b{-}W)$ with the $\nu_{as}(W{-}O_c{-}W)$ vibrational bands. Therefore, we assign the broader band at 790 cm^{-1} to contributions from both $\nu_{as}(W{-}O_b{-}W)$ and $\nu_{as}(W{-}O_c{-}W)$ vibrations whose SERS comes from the fact that there are at least two $W{-}O_b{-}W$ and two $W{-}O_c{-}W$ bonds that are quite close to the surface ($\sim$0.5 nm) and perpendicular to the Ag NP surface.

We show in Fig. 5 the time-dependent SERS spectra (A) of the lacunary $SiW_{11}O_{39}^{8-}$ anions (2.5 mM) adsorbing onto the Ag NP surfaces and the corresponding UV-Vis SPR spectra (B) of the Ag NPs. Similar to the $PW_{11}O_{39}^{7-}$ anions, an almost complete displacement of the metal-surface-bound citrate ions took place right after the addition of the $SiW_{11}O_{39}^{8-}$ anions, accompanied by an immediate red-shift (389–396 nm) in the surface plasma peak (Fig. 5B) and the appearance of SERS peaks at 960 and 789 cm^{-1} (Fig. 5A). The overall behaviors are the same as those observed on the adsorbed $PW_{11}O_{39}^{7-}$ anions, in particular a red shift

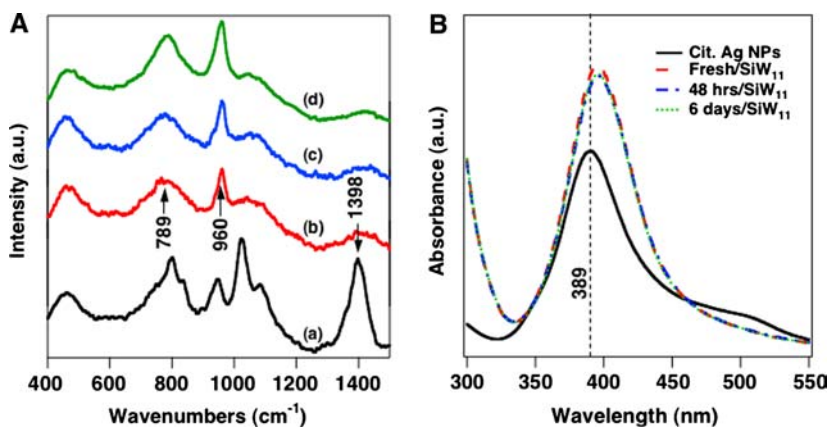**Fig. 5.** The time-dependent SERS (A) and UV-Vis SPR (B) spectra of the Ag–citrate and Ag NP–$SiW_{11}O_{39}^{8-}$ samples. A/B: (a)/solid curves: Ag–citrate; (b)/dashed curves: right after, (c)/dash-dotted curves: 48 h after, and (d)/dotted curves: 6 days after the addition of the SiW_{11}.

of the SERS $\nu_s(W=O_d)$ band at 960 cm^{-1} with respect to that (978 cm^{-1}) of the free $SiW_{11}O_{39}^{8-}$ and the broader SERS band at 789 cm^{-1}. Thus, we believe that the $SiW_{11}O_{39}^{8-}$ assumes the same bonding configuration as proposed in Fig. 4. However, the amplitude of the SERS signals from the adsorbed POM changes only slightly after the addition of the POM and the peak at 789 cm^{-1} is much broader than its counterpart observed in the adsorbed $PW_{11}O_{39}^{7-}$. Accordingly, the color of the solution as well as the surface plasma peak do not change after the initial variations (Fig. 5B). These differences suggest that the Ag–$SiW_{11}O_{39}^{8-}$ may have higher bonding disorder and better overall stability.

However, increasing the concentration of the $SiW_{11}O_{39}^{8-}$ induces instability, though the kinetic of the POM adsorption seemed to be enhanced. Figure 6 presents a series of SERS spectra as a function of time when the concentration of the added $SiW_{11}O_{39}^{8-}$ was increased from 2.5 to 5 mM that led to the eventual precipitation of the colloidal Ag NP solution. As can be seen, as the precipitation happened as indicated by the appearance of the black Ag, the SERS signals decreased and eventually led to the Raman spectrum of a free POM solution. The exactly same Raman spectrum of the precipitated solution as that of a free POM solution again strongly indicates that the overall molecular structure of the POM was intact when adsorbed on the Ag NPs.
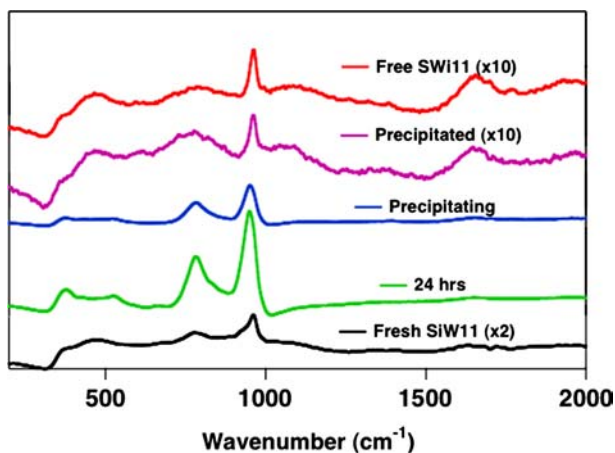
Fig. 6. The time-dependent SERS spectra after the concentration of the added $SiW_{11}O_{39}^{8-}$ was increased from 2.5 to 5 mM that led the eventual precipitation of the solution.

CONCLUSIONS

We have reported the first rather detailed SERS investigation of the interactions between the Keggin-type lacunary POMs and the colloidal Ag NPs. Several important conclusions can be reached. First, the observed displacement of the pre-existing citrate ions demonstrates unambiguously a stronger chemical bonding interaction between the POMs and the Ag NPs than between the citrate ions and the Ag NPs. Second, the SERS spectroscopic evidence indicates that the lacunary POMs bind to the Ag NP surface via the penta-dentate aperture with 5 oxygen atoms directly bound to the surface. A similar bonding scheme has been proposed for interactions between $SiW_{11}O_{39}^{8-}$ and single crystal Ag surface [19]. Third, the simultaneous observation of several SERS bands attributable to the POM molecules suggests that the overall molecular structure of the adsorbed POMs is largely intact. And fourth, the high quality SERS spectra observed have clearly demonstrated the promising potential of the powerful SERS spectroscopy to investigate metal NP based POM surface chemistry.

ACKNOWLEDGMENTS

authors gratefully thank Professors M. Pope and N. Belai for providing POMs used in this study and for fruitful discussions.

REFERENCES

1. M. T. Pope, *Heteropoly and Isopoly Oxometalates* (Springer-Verlag, New York, 1983).
2. D. E. Katsoulis (1998). *Chem. Rev.* **98**, 359.
3. W. B. Kim, T. Voitl, G. J. Rodriguez-Rivera, S. T. Evans, and J. A. Dumesic (2005). *Ange. Chem. Int. Ed.* **44**, 778.
4. W. B. Kim, T. Voitl, G. J. Rodriguez-Rivera, and J. A. Dumesic (2004). *Science* **305**, 1280.
5. S. V. Lomakina, T. S. Shatova, and L. P. Kazansky (1994). *Corr. Sci.* **36**, 1645.
6. A. Troupis, A. Hiskia, and E. Papaconstantinou (2002). *Angewandte Chemie: International Edition in English* **41**.
7. Y. Lin and R. G. Finke (1994). *J. Am. Chem. Soc.* **116**, 8335.
8. J. D. Aiken III and R. G. Finke (1999). *Chem. Mater.* **11**, 1035.
9. A. V. Gordeev and B. G. Ershov (1999). *High Energy Chem.* **33**, 218.
10. S. Mandal, P. Selvakannan, R. Pasricha, and M. Sastry (2003). *J. Am. Chem. Soc.* **125**, 8440.
11. S. Mandal, A. Das, R. Srivastava, and M. Sastry (2005). *Langmuir* **21**, 2408.
12. S. Ozkar and R. G. Finke (2002). *J. Am. Chem. Soc.* **124**, 5796.
13. A. Kuhn and F. C. Anson (1996). *Langmuir* **12**, 5481.
14. C.-Y. Rong and F. C. Anson (1996). *Inorg. Chim. Acta* **242**, 11.
15. W. G. Klemperer and C. G. Wall (1998). *Chem. Rev.* **98**, 297.
16. M. H. Ge, B. X. Zhong, W. G. Klemperer, and A. A. Gewirth (1996). *J. Am. Chem. Soc.* **118**, 5812.
17. L. Lee, J. X. Wang, R. R. Adzic, I. K. Robinson, and A. A. Gewirth (2001). *J. Am. Chem. Soc.* **123**, 8838.
18. C. M. Teague, X. Li, M. E. Biggin, L. Lee, J. Kim, and A. A. Gewirth (2004). *J. Phys. Chem. B* **108**, 1974.
19. J. Kim and A. A. Gewirth (2003). *Langmuir* **19**, 8934.
20. J. Turkevich and G. Kim (1970). *Science* **169**, 873.
21. A. M. Ahern and R. L. Garrell (1987). *Anal. CVhem.* **59**, 2813.
22. O. Silman, L. A. Bumm, R. Callaghan, C. G. Blatchford, and M. Kerker (1983). *J. Phys. Chem.* **87**, 1014.
23. N. R. Jana, L. Gearheart, and C. J. Murphy (2001). *Chem. Commun.* 617.
24. C. Rocchiccioli-Deltcheff and R. Thouvenot (1977). *J. Chem. Res. (S)* 46.
25. M. Moskovits (1985). *Rev. Mod. Phys.* **57**, 783.
26. C. L. Hayne, A. D. McFarland, and R. P. Duynevan (2005). *Anal. Chem.* **77**, 338A.
27. S. J. Lee, A. R. Morrill, and M. Moskovits (2006). *J. Am. Chem. Soc.* **128**, 2200.